

## Negative space charge effects in photon-enhanced thermionic emission solar converters

G. Segev, D. Weisman, Y. Rosenwaks, and A. Kribus

Citation: [Applied Physics Letters](#) **107**, 013908 (2015); doi: 10.1063/1.4926625

View online: <http://dx.doi.org/10.1063/1.4926625>

View Table of Contents: <http://scitation.aip.org/content/aip/journal/apl/107/1?ver=pdfcov>

Published by the [AIP Publishing](#)

---

### Articles you may be interested in

[Thermodynamics of photon-enhanced thermionic emission solar cells](#)

*Appl. Phys. Lett.* **104**, 023902 (2014); 10.1063/1.4862535

[Loss mechanisms and back surface field effect in photon enhanced thermionic emission converters](#)

*J. Appl. Phys.* **114**, 044505 (2013); 10.1063/1.4816256

[Optically pumped cesium plasma neutralization of space charge in photon-enhanced thermionic energy converters](#)

*Appl. Phys. Lett.* **101**, 213901 (2012); 10.1063/1.4767349

[Diffusion-emission theory of photon enhanced thermionic emission solar energy harvesters](#)

*J. Appl. Phys.* **112**, 044506 (2012); 10.1063/1.4747905

[Development of a cylindrical inverted thermionic converter for solar power systems](#)

*AIP Conf. Proc.* **504**, 1302 (2000); 10.1063/1.1290943

---



Frustrated by old technology? Is your AFM dead and can't be repaired? Sick of bad customer support?

**It is time to upgrade your AFM**  
Minimum \$20,000 trade-in discount for purchases before August 31st

**Asylum Research is today's technology leader in AFM**

dropmyoldAFM@oxinst.com

**OXFORD INSTRUMENTS**  
The Business of Science®

The advertisement features three images: an old AFM, a tombstone for 'My Old AFM 1994-2015', and a frustrated man. The background is dark blue with white and orange text.

## Negative space charge effects in photon-enhanced thermionic emission solar converters

G. Segev,<sup>1</sup> D. Weisman,<sup>1</sup> Y. Rosenwaks,<sup>1</sup> and A. Kribus<sup>2,a)</sup>

<sup>1</sup>School of Electrical Engineering, Faculty of Engineering, Tel-Aviv University, Tel Aviv 69978, Israel

<sup>2</sup>School of Mechanical Engineering, Faculty of Engineering, Tel-Aviv University, Tel Aviv 69978, Israel

(Received 26 March 2015; accepted 29 June 2015; published online 10 July 2015)

In thermionic energy converters, electrons in the gap between electrodes form a negative space charge and inhibit the emission of additional electrons, causing a significant reduction in conversion efficiency. However, in Photon Enhanced Thermionic Emission (PETE) solar energy converters, electrons that are reflected by the electric field in the gap return to the cathode with energy above the conduction band minimum. These electrons first occupy the conduction band from which they can be reemitted. This form of electron recycling makes PETE converters less susceptible to negative space charge loss. While the negative space charge effect was studied extensively in thermionic converters, modeling its effect in PETE converters does not account for important issues such as this form of electron recycling, nor the cathode thermal energy balance. Here, we investigate the space charge effect in PETE solar converters accounting for electron recycling, with full coupling of the cathode and gap models, and addressing conservation of both electric and thermal energy. The analysis shows that the negative space charge loss is lower than previously reported, allowing somewhat larger gaps compared to previous predictions. For a converter with a specific gap, there is an optimal solar flux concentration. The optimal solar flux concentration, the cathode temperature, and the efficiency all increase with smaller gaps. For example, for a gap of  $3\ \mu\text{m}$  the maximum efficiency is 38% and the optimal flux concentration is 628, while for a gap of  $5\ \mu\text{m}$  the maximum efficiency is 31% and optimal flux concentration is 163. © 2015 Author(s). All article content, except where otherwise noted, is licensed under a Creative Commons Attribution 3.0 Unported License. [<http://dx.doi.org/10.1063/1.4926625>]

Thermionic emission was studied extensively in the 1970s as means to convert heat directly to electricity. The conversion process is based on emission of electrons from the surface of a high temperature cathode, and their subsequent collection in a lower temperature anode, separated by a vacuum or low pressure gap.<sup>1</sup> Positive output voltage and output power are achieved by appropriate selection of the work functions of both surfaces. However, such converters require cathode temperatures significantly above  $1000\ ^\circ\text{C}$ , and even at these high temperatures, their conversion efficiency is below 20%, and therefore, they are not widely implemented.

In Photon Enhanced Thermionic Emission (PETE) converters, the cathode is made of a semiconductor material and is illuminated with above band gap photons, for example, from concentrated sunlight.<sup>2</sup> Optical generation of conduction band electrons increases the cathode's conduction band electron concentration and raises the conduction band quasi-Fermi level.

As a result, the effective barrier for electron emission is reduced, allowing electron emission at temperatures considerably lower than in standard thermionic emission. The excess photon energy above the band gap is passed to the lattice through thermalization, leading to increased cathode temperature and higher efficiency.<sup>3</sup> Therefore, some of the heat generated by thermalization is converted to electrical

power. The energy of sub-bandgap photons can also contribute to increase the temperature and the conversion efficiency, if the cathode contains an IR coupling element that absorbs them. The thermal contribution to the conversion process raises the PETE efficiency above the Shockley Queisser limit for single junction solar cells, theoretically reaching around 50%.<sup>2,4</sup> Waste heat removed from the anode can drive a secondary heat-to-electricity converter stage, theoretically approaching overall efficiency of 70% under concentration of 1000 sun.<sup>5</sup>

The electrons emitted from the cathode of a thermionic converter require a finite time to reach the anode, and therefore a negatively charged electron cloud forms in the inter-electrode space. This negative space charge produces an added potential barrier that impedes the emitted electrons from reaching the anode. The loss inflicted by the negative space charge was shown to be quite high in thermionic converters.<sup>6</sup> Reducing the gap between the electrodes diminishes the negative space charge and with it the negative space charge loss. However, for gaps below  $1\ \mu\text{m}$ , near field radiation forms a thermal shunt between the two electrodes, once again reducing the converter efficiency.<sup>7</sup> Another approach to reduce the negative space charge loss is to introduce positive charges in the gap, which cancel the effect of the negative charge. Filling the gap with low pressure cesium vapor forms such positively charged plasma in the gap.<sup>1</sup> Denser plasma can be formed by optically exciting the cesium, lowering its effective ionization potential, and canceling the negative space charge more effectively.<sup>8</sup> Methane also reduces

<sup>a)</sup>Author to whom correspondence should be addressed. Electronic mail: [kribus@tauex.tau.ac.il](mailto:kribus@tauex.tau.ac.il)



the negative space charge loss in a similar manner, and introduces molecular charge transport as well.<sup>9</sup> Incorporation of a positively charged grid between the two electrodes to accelerate the emitted electrons can also reduce negative space charge loss.<sup>10</sup> Using negative electron affinity cathodes is also beneficial, as the emitted electrons leave the cathode with energy higher than the vacuum level at the surface, and are better equipped to overcome the negative space charge energy barrier.<sup>11</sup> The current study refers to the simplest converter configuration with just vacuum in the gap between the two electrodes. The theory presented here can be further expanded in the future, to account for additional effects that modify charge transport in the gap.

In PETE devices, electrons that are reflected by the electric field in the gap return to the cathode with an energy which is at least the vacuum level at the cathode emitting surface. As a result, once reabsorbed in the cathode, these electrons will first populate the conduction band from which they can be reemitted or recombined. This form of electron recycling was shown to have a significant effect on the performance of ideal PETE converters where negative space charge effects are not considered. It shifts the maximum power point voltage to voltages above the difference in the electrodes work functions, it allows the efficiency to increase monotonically with temperature, and it makes lower cathode electron affinities more favorable.<sup>3</sup> A recently published analysis of negative space charge effect in PETE converters<sup>12</sup> presented the basic theory, but failed to consider the dependence of the cathode conduction band electron concentration on the operating voltage, which is essential in order to account for the electron recycling mechanism. Therefore, the coupling of the cathode model to the negative space charge model was incomplete, with a missing feedback connection from the negative space charge to the cathode. In this work, we present a more complete model that accounts for this missing effect to provide full two-way coupling of the cathode and negative space charge models, and considers conservation of both electric and thermal energy.

In order to fully account for the variation of the conduction electrons concentration with the operating voltage, which represents the electron recycling mechanism due to negative space charge, the cathode particle balance and the negative space charge models must be coupled. The cathode particle balance<sup>2,3</sup> allows calculating the cathode electrons concentration and emission current as a function of the materials properties (cathode doping, band gap, electron affinity, and anode work function), operating conditions (flux concentration and temperature), and the potential barrier between the electrodes. The negative space charge model as described in Refs. 1 and 6 yields the potential barrier imposed by the negative space charge for a given set of operating conditions, emission current, and material properties. The two models are coupled by assuming current and field continuity, i.e., that all the electrons emitted from the cathode surface enter the gap and that there are no trapped charges at this surface. Coupling the two models' equation sets is done by passing the potential barrier caused by the negative space charge to the particle balance, and the emission current, which is the result of the particle balance, back to the negative space charge model. Repeating this procedure at every operating voltage allows calculating complete current voltage

curves accounting for both mechanisms. The coupling of the two models can be done with simple nonlinear equation solver. For convenience, a detailed description of the models and an example for a coupling method using an iterative numerical procedure can be found in the supplementary material.<sup>13</sup> Once the current voltage curve is found, the corresponding conversion efficiency,  $\eta$ , follows:  $\eta = J_{mpp} \cdot V_{mpp} / P_{in}$ , where  $J_{mpp}$  is the maximum power point net current density,  $V_{mpp}$  is the maximum power point voltage, and  $P_{in}$  is the incident solar power flux. The following parameters were used in all the results reported below unless stated otherwise. The cathode is a doped p-type semiconductor with acceptors concentration of  $10^{19} \text{ cm}^{-3}$  and a bandgap of 1.4 eV.<sup>2</sup> The electron and hole effective masses are  $m_e$  and  $0.57 m_e$ , respectively, where  $m_e$  is the free electron mass.<sup>14</sup> The anode temperature is 500 K and its work function is 0.9 eV.<sup>15</sup> The cathode is assumed to be ideal in the sense that all incident photons with above band gap energy are absorbed and there are no potential drops within the cathode. Only radiative recombination is considered; the possible impact of surface and Shockley-Reed-Hall (SRH) recombination is discussed below and in the supplementary material.<sup>13</sup> The incident radiation is the AM1.5D spectrum multiplied by the flux concentration and added to the diffuse spectrum. Near field radiative heat transfer between the electrodes was not considered. However, this mechanism is negligible for gaps above  $1 \mu\text{m}$ .<sup>7</sup> Unless stated otherwise, the cathode temperature is 760 K. The photo-enhancement of electron emission leads to the assumed condition where the cathode emission current is significantly higher than the anode reverse emission even at this relatively low cathode temperature. The PETE device operates in the PETE regime in the entire range of cathode temperatures, i.e., the emission current is mostly determined by the incident photons concentration rather than the cathode temperature.

Figure 1 shows current-voltage curves for PETE devices influenced by negative space charge for two gap widths of  $2 \mu\text{m}$  and  $5 \mu\text{m}$ , compared to the same results using the no

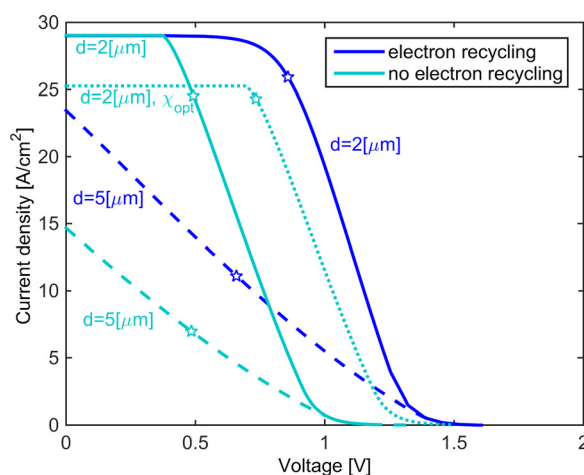


FIG. 1. Current-voltage characteristics of PETE converters subject to negative space charge, with  $T_C = 760 \text{ K}$ ,  $\chi = 0.4 \text{ eV}$ , and concentration ratio  $1000\times$ . Stars show the maximum power point for each curve. The cathode is a doped p-type semiconductor with acceptors concentration of  $10^{19} \text{ cm}^{-3}$  and a band gap of 1.4 eV. The electron and hole effective masses are  $m_e$  and  $0.57 m_e$ , respectively. The anode temperature is 500 K, and its work function is 0.9 eV. Also shown is the current voltage curve calculated with the no electron recycling model using its optimal electron affinity,  $\chi_{opt} = 0.68 \text{ eV}$ , for this set of operating conditions.

electron recycling model.<sup>12</sup> The flux concentration is 1000, and the cathode electron affinity is 0.4 eV. The maximum power points are marked with stars and are all within the space charge limited range. The efficiencies calculated with the electron recycling model are 24.7% and 8.1% for gap widths of 2  $\mu\text{m}$  and 5  $\mu\text{m}$ . The efficiencies calculated with the no electron recycling model are 13.4% and 3.8% for gap widths of 2  $\mu\text{m}$  and 5  $\mu\text{m}$ . Comparing to the no electron recycling model, the present model predicts a more gradual decrease in current with increasing voltage. This leads to a significant difference in the location of the maximum power point and in the efficiency predicted by the two models. This is similar to the results of a previous comparison between the two models, where negative space charge effects were absent.<sup>3</sup> The mechanism behind this difference is that emitted electrons that are reflected by the negative space charge electric field are reabsorbed and thermalized in the cathode. This increases the conduction band population, and significantly increases the emitted current in the crucial operation region that contains the maximum power point of the converter. As a result, the decrease of current and power output with voltage is less severe than the prediction of the no electron recycling model, and the maximum power and efficiency are higher.

When negative space charge effects are not considered, the efficiency calculated with the electron recycling and no electron recycling models converge at the optimal electron affinity predicted by the no electron recycling model.<sup>3</sup> At this optimal affinity value, the maximum power point voltage in the electron recycling model is exactly the difference in work functions and the two models predict the same efficiency. However, in the presence of negative space charge, the maximum power point is lower than the difference in work functions, and the no electron recycling model efficiency prediction is lower. Figure 1 also shows the current voltage curve calculated with the no electron recycling model with an electron affinity of 0.68 which is the optimal electron affinity,  $\chi_{opt}$ , for these operating conditions. The efficiency in this case is 19.8%, compared to about 24% for the electron recycling model, which is nearly constant for electron affinity in the range of 0–0.7 eV.

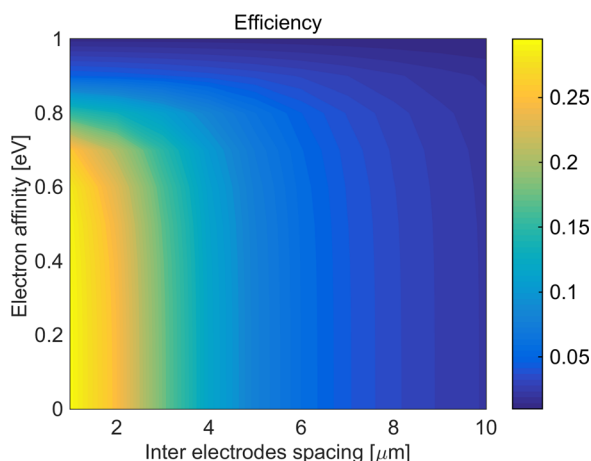


FIG. 2. Efficiency as a function of inter-electrode spacing and electron affinity. All the other simulation parameters are as in Figure 1.

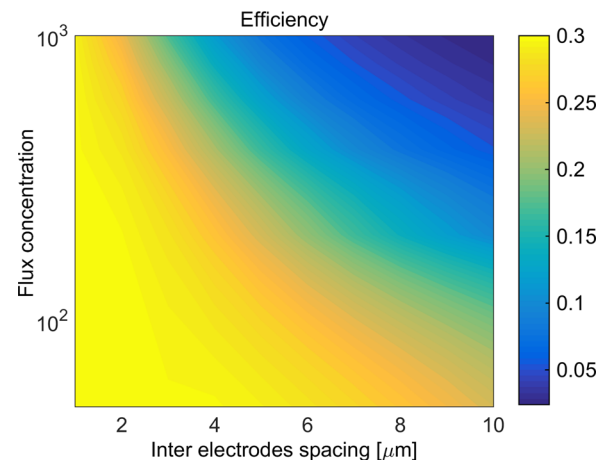


FIG. 3. Efficiency as a function of inter-electrode spacing and flux concentration, where all other parameters are as in Figure 1.

Figure 2 shows the efficiency as a function of the inter-electrode spacing and the cathode electron affinity. As discussed above, the efficiency decreases significantly when the inter-electrode spacing increases. The efficiency is nearly independent of the electron affinity up to 0.65 eV, in contrast to the no electron recycling model<sup>12</sup> that predicts an optimum value of the electron affinity for every cathode temperature. For electron affinity above 0.65 eV, the efficiency decreases rapidly. Efficiencies above 20% can be achieved with spacing of up to 2  $\mu\text{m}$  and electron affinity below 0.7 eV, and reducing the gap to 1  $\mu\text{m}$  yields an efficiency of about 30%. This efficiency is lower than the maximum efficiencies reported in Refs. 2 and 3 because of the moderate cathode temperature used in this example.

Figure 3 shows the efficiency as a function of the solar flux concentration and the inter-electrode spacing. For high concentration, the current density is high leading to significant negative space charge effect, requiring a very small gap below 2  $\mu\text{m}$  to achieve high efficiency close to 30%. For lower concentration, the current density and the negative space charge effect are smaller, allowing high efficiency at larger spacing.

Figure 4 shows the conversion efficiency as a function of the cathode temperature and gap width. The efficiency

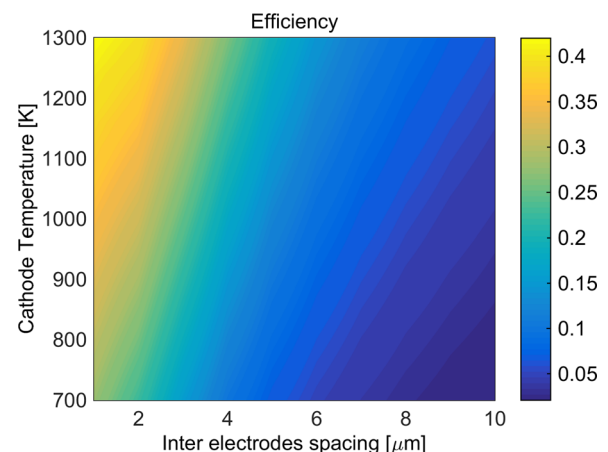


FIG. 4. Efficiency as a function of the inter electrode spacing and cathode temperature, where all other parameters are as in Figure 1.

increases with the cathode temperature for all inter-electrodes spacings. Since the device operates in the PETE regime for the entire temperature range presented, the cathode saturation current is determined by the photo-generation rate and hardly changes with the cathode temperature.<sup>16</sup> Hence, the added barrier due to negative space charge does not increase with temperature, and the efficiency can increase with temperature. These results are again in contrast to the no electron recycling model,<sup>12</sup> which predicts an optimal temperature for each gap size. It should be noted that the transition temperature between the PETE regime and thermionic regimes is very sensitive to the cathode contact properties. In this work, we assume a perfectly selective cathode contact. As a result, the transition from the PETE to the thermionic regime is at temperatures above the shown range. Nonideal contacts as discussed in Refs. 16 and 17 will lead to a regime transition at lower temperatures. As a result, higher current densities will occur at lower temperatures, leading to higher negative space charge loss.

The cathode temperature is not an independent variable, but rather it is determined by the flux concentration according to the energy balance of the cathode, as described in the supplementary material.<sup>13</sup> Increasing the concentration increases the temperature, leading to conflicting effects on the conversion efficiency, as discussed above. Therefore, an optimal concentration may exist. Figure 5 shows the efficiency and cathode temperature as a function of the concentration for several values of inter-electrodes spacing, subject to the energy balance that determines the cathode temperature. For a gap of  $1\ \mu\text{m}$ , negative space charge has little effect on the device performance, and the efficiency and temperature converge to the results of Ref. 3 that do not account for negative space charge. The efficiency in this case reaches nearly 45% at flux concentration of 1000, and the cathode temperature is 1405 K. For larger gaps, the negative space charge effect is more significant, and its impact is visible at the higher concentrations where the current density and the negative space charge barrier are higher. This leads to an optimal flux concentration, above which the negative space

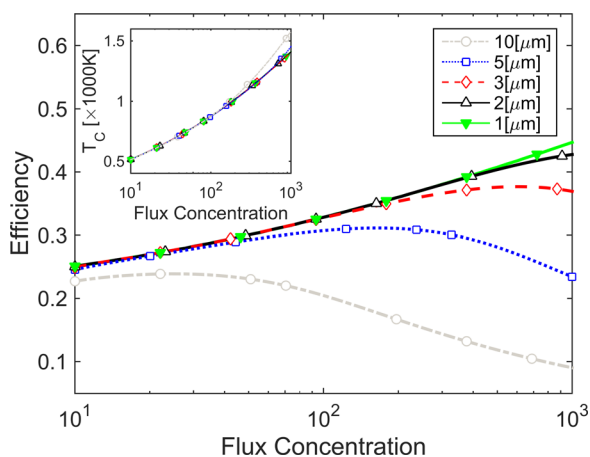


FIG. 5. PETE converter efficiency as a function of the flux concentration. The cathode is subject to an energy balance and is operating at the maximum power point. The inset shows the corresponding cathode temperature. All converter parameters are as in Figure 1.

charge loss dominates and the efficiency decreases. As the gap width increases, the negative space charge effect is stronger, and the optimal concentration and the maximum efficiency both diminish. For example, for gaps of  $3\ \mu\text{m}$ ,  $5\ \mu\text{m}$ , and  $10\ \mu\text{m}$ , the peak efficiencies occur at concentrations of 600, 170, and 25, respectively. The corresponding efficiencies are 0.38, 0.31, and 0.24, respectively. A side effect of the reduction in emitted current due to negative space charge is an increase in cathode temperature, since less power leaves the cathode with emitted electrons. The inset in Figure 5 shows this effect under high concentration as a temperature rise with higher interelectrode spacing.

Surface recombination at the emitting surface was shown to have a drastic effect on the PETE conversion efficiency.<sup>18–20</sup> Since this work is concerned with the performance of ideal PETE cathodes, recombination mechanisms that originate from defect states such as surface and SRH recombination were not considered. It should be noted that since the model is based on a net particle balance, it cannot discriminate between recombination at the cathode bulk vs. the emitting surface. In order to analyze the impact of these effects, it is possible to assign both SRH and surface recombination an effective recombination velocity. However, this added recombination will not only reduce the number of electrons that can be recycled, i.e., reemit to the vacuum after being reflected by the space charge, but will also reduce the emission current at voltages below the saturation voltage. For this reason, the model without electron recycling (constant electron concentration<sup>12</sup>) describes a non-trivial form of electron capture, which is not simple surface recombination. A detailed discussion of the surface and SRH recombination effects can be found in the supplementary material.<sup>13</sup>

The current model with a more complete coupling of the cathode and gap models shows that the efficiency increases monotonically with increasing temperature and declining cathode electron affinity, unlike the prediction of previous models. The model predicts an optimal flux concentration for each inter-electrode spacing width. For gaps below  $2\ \mu\text{m}$ , the negative space charge effect is small for flux concentration as high as 1000. However, for large gaps, the optimal flux concentration and the highest achievable efficiency decline dramatically. Therefore, the technological ability to produce closely spaced electrodes may determine the choice of optics and other system elements. For example, if technical limitations lead to a practical gap width of  $10\ \mu\text{m}$ , this defines an optimal flux concentration of only 25, and a simple linear solar concentrator with single axis tracking will suffice. Obviously, this model does not consider the other methods described above for reducing the negative space charge loss, which may allow larger gaps without limiting the concentration.

This work was supported by the European Union's Seventh Framework Programme for research, technological development and demonstration under Grant Agreement No: 308975 (Project PROMETHEUS, <http://www.prometheus-energy.eu/>). G. Segev acknowledges the support of Eshkol fellowship from the Israel Ministry of Science and Technology.

- <sup>1</sup>G. N. Hatsopoulos and E. P. Gyftopoulos, *Thermionic Energy Conversion Vol. 1: Processes and Devices* (MIT Press, Cambridge, MA, USA, 1973).
- <sup>2</sup>J. W. Schwede, I. Bargatin, D. C. Riley, B. E. Hardin, S. J. Rosenthal, Y. Sun, F. Schmitt, P. Pianetta, R. T. Howe, Z.-X. Shen, and N. A. Melosh, *Nat. Mater.* **9**, 762 (2010).
- <sup>3</sup>G. Segev, Y. Rosenwaks, and A. Kribus, *Sol. Energy Mater. Sol. Cells* **107**, 125 (2012).
- <sup>4</sup>G. Segev, Y. Rosenwaks, and A. Kribus, *AIP Conf. Proc.* **53**, 53 (2013).
- <sup>5</sup>G. Segev, Y. Rosenwaks, and A. Kribus, *Sol. Energy Mater. Sol. Cells* **140**, 464 (2015).
- <sup>6</sup>J. R. Smith, G. L. Bilbro, and R. J. Nemanich, *J. Vac. Sci. Technol., B* **27**, 1132 (2009).
- <sup>7</sup>J.-H. Lee, I. Bargatin, N. A. Melosh, and R. T. Howe, *Appl. Phys. Lett.* **100**, 173904 (2012).
- <sup>8</sup>T. Ito and M. A. Cappelli, *Appl. Phys. Lett.* **101**, 213901 (2012).
- <sup>9</sup>F. A. M. Koeck, R. J. Nemanich, Y. Balasubramaniam, K. Haenen, and J. Sharp, *Diamond Relat. Mater.* **20**, 1229 (2011).
- <sup>10</sup>S. Meir, C. Stephanos, T. H. Geballe, and J. Mannhart, *J. Renewable Sustainable Energy* **5**, 043127 (2013).
- <sup>11</sup>J. R. Smith, G. L. Bilbro, and R. J. Nemanich, *Diamond Relat. Mater.* **15**, 2082 (2006).
- <sup>12</sup>S. Su, Y. Wang, T. Liu, G. Su, and J. Chen, *Sol. Energy Mater. Sol. Cells* **121**, 137 (2014).
- <sup>13</sup>See supplementary material at <http://dx.doi.org/10.1063/1.4926625> for further details on the analysis, numerical procedure, and the effective recombination velocity effects.
- <sup>14</sup>S. M. Sze, *Physics of Semiconductor Devices* (Wiley, 2007).
- <sup>15</sup>F. A. M. Koeck, R. J. Nemanich, A. Lazea, and K. Haenen, *Diamond Relat. Mater.* **18**, 789 (2009).
- <sup>16</sup>G. Segev, Y. Rosenwaks, and A. Kribus, *J. Appl. Phys.* **114**, 044505 (2013).
- <sup>17</sup>R. Sandovsky, G. Segev, Y. Rosenwaks, and A. Kribus, in *29th European Photovoltaic Solar Energy Conference and Exhibition* (Amsterdam, 2014), pp. 43–45.
- <sup>18</sup>A. Varpula and M. Prunnila, *J. Appl. Phys.* **112**, 044506 (2012).
- <sup>19</sup>K. Sahasrabudde, J. W. Schwede, I. Bargatin, J. Jean, R. T. Howe, Z.-X. Shen, and N. A. Melosh, *J. Appl. Phys.* **112**, 094907 (2012).
- <sup>20</sup>J. W. Schwede, T. Sarmiento, V. K. Narasimhan, S. J. Rosenthal, D. C. Riley, F. Schmitt, I. Bargatin, K. Sahasrabudde, R. T. Howe, J. S. Harris, N. A. Melosh, and Z.-X. Shen, *Nat. Commun.* **4**, 1576 (2013).